8-8-2018

Neonatal lactocrine deficiency affects the adult porcine endometrial transcriptome at pregnancy day 13

Ashley F. George
Rutgers University

Teh-Yuan Ho
Rutgers University

Nripesh Prasad
HudsonAlpha Institute for Biotechnology

Brittney N. Keel
U.S. Meat Animal Research Center (USMARC)

Jeremy R. Miles
U.S. Meat Animal Research Center (USMARC), jeremy.miles@usda.gov

See next page for additional authors

Biology of Reproduction, 2019, 100(1), 71–85
doi:10.1093/biolre/ioy180
Research Article
Advance Access Publication Date: 9 August 2018

OXFORD

Research Article

Neonatal lactocrine deficiency affects the adult porcine endometrial transcriptome at pregnancy day 13†

Ashley F. George[1], Teh-Yuan Ho[1], Nripesh Prasad[2], Brittney N. Keel[3], Jeremy R. Miles[3], Jeffrey L. Vallet[3], Frank F. Bartol[4,‡] and Carol A. Bagnell[1,*,‡]

[1]Department of Animal Sciences, Endocrinology and Animal Biosciences Program, Rutgers University, New Brunswick, New Jersey, USA; [2]HudsonAlpha Institute for Biotechnology, Huntsville, Alabama, USA; [3]USDA, ARS, U.S. Meat Animal Research Center (USMARC), Clay Center, Nebraska, USA and [4]Department of Anatomy, Physiology and Pharmacology, Cellular and Molecular Biosciences Program, Auburn University, Auburn, Alabama, USA

*__Correspondence__: Department of Animal Sciences, Rutgers University, 84 Lipman Drive, New Brunswick, NJ 08901, USA. E-mail: cbagnell@sebs.rutgers.edu

†__Grant support:__ This work is supported by USDA-NRI-2013-67016-20523 (to FFB and CAB), NSF- EPS-1158862 (to FFB) and the Steinetz Charitable Lead Unitrust (to CAB). Sequencing data were deposited in the Gene Expression Omnibus (GEO) repository under series accession number GSE113518.
‡Joint senior authors

Received 1 June 2018; Revised 19 July 2018; Accepted 8 August 2018

Abstract

Reproductive performance of female pigs that do not receive sufficient colostrum from birth is permanently impaired. Whether lactocrine deficiency, reflected by low serum immunoglobulin immunocrit (iCrit), affects patterns of endometrial gene expression during the periattachment period of early pregnancy is unknown. Here, objectives were to determine effects of low iCrit at birth on the adult endometrial transcriptome on pregnancy day (PxD) 13. On the first day of postnatal life, gilts were assigned to high or low iCrit groups. Adult high (n = 8) and low (n = 7) iCrit gilts were bred (PxD 0), and humanely slaughtered on PxD 13 when tissues and fluids were collected. The endometrial transcriptome was defined for each group using mRNAseq and microRNAseq. Reads were mapped to the *Sus scrofa* 11.1 genome build. Mature microRNAs were annotated using miRBase 21. Differential expression was defined based on fold change ($\geq \pm 1.5$). Lactocrine deficiency did not affect corpora lutea number, uterine horn length, uterine wet weight, conceptus recovery, or uterine luminal fluid estrogen content on PxD 13. However, mRNAseq revealed 1157 differentially expressed endometrial mRNAs in high versus low iCrit gilts. Differentially expressed genes had functions related to solute transport, endometrial receptivity, and immune response. Six differentially expressed endometrial microRNAs included five predicted to target 62 differentially expressed mRNAs, affecting similar biological processes. Thus, lactocrine deficiency on the first day of postnatal life can alter uterine developmental trajectory with lasting effects on endometrial responses to pregnancy as reflected at the level of the transcriptome on PxD 13.

Summary Sentence

Lactocrine deficiency on the first day of postnatal life alters the uterine developmental program with long-term effects on patterns of porcine endometrial gene expression during the periattachment period of early pregnancy.

Key words: domestic animal reproduction, endometrium, gene expression, implantation, microRNA, porcine/pig, pregnancy, uterus.

Introduction

The mammalian female reproductive tract is incompletely developed at birth (postnatal day = PND 0) [1]. Data for ungulates [2–4] and mice [5, 6] showed that transient disruption of neonatal uterine development can alter the postnatal developmental program with lasting consequences for adult uterine structure and function. Thus, neonatal uterine tissues are developmentally plastic. Moreover, conditions necessary to support an optimal uterine developmental trajectory are not well defined. Disruption of such conditions, resulting in suboptimal development, can compromise the ability of adult uterine tissues to support pregnancy and, for polytocous species, to produce large, viable litters.

Maternal support of offspring development does not end at birth, but extends into the postnatal period through factors communicated from mother to nursing young in first milk (colostrum) via a lactocrine mechanism [7, 8]. In the pig (*Sus scrofa*), studies designed to test the lactocrine hypothesis for maternal programming of postnatal uterine development showed that imposition of a lactocrine-null state for 2 days from birth by feeding milk replacer in lieu of nursing altered uterine gene expression on PND 2 [9–11], and stunted endometrial gland development by PND 14 [11]. Observations indicated a requirement for lactocrine support of the neonatal uterine developmental program.

Lactocrine deficiency from birth, defined as suboptimal delivery of milk-borne bioactive factors to nursing young, also occurs under nonexperimental conditions. In the pig, lactocrine deficiency can occur naturally through sow (e.g. maternal agalactia, mastitis) or piglet-based factors (e.g. difficulty during the birth process, low birth weight, competition among nursing young for teat position) [12–14]. The serum immunoglobulin immunocrit (iCrit) assay [15], used to monitor passive transfer of maternal immunoglobulin to nursing piglets, provides an indirect method for assessing the relative amount of colostrum acquired by neonates on their first day after birth. In pigs, minimal colostrum consumption on the day of birth (PND 0), reflected by low serum iCrit values within the first 24 h of postnatal life, not only altered patterns of uterine wall development in neonates by PND 14 [8], but also reduced live litter size through four parities in lactocrine-deficient piglets that reached adulthood [14]. Results provided compelling evidence indicating that reproductive performance of adult, neonatally lactocrine-deficient female pigs is permanently impaired [14].

Factors that disrupt uterine receptivity to implantation of blastocysts during the periattachment period can compromise reproductive performance [16]. In the pig, conceptus elongation typically starts on day 11 and trophoblast attachment to the uterine luminal epithelium occurs starting on pregnancy day (PxD) 13, and is completed by PxD 18 [17]. During this period, uterine secretions support developing conceptuses, and functional changes in the endometrium facilitate implantation [18, 19]. These events contribute to establishment of an embryotrophic intrauterine environment that evolves as pregnancy progresses.

Significant changes in patterns of endometrial gene expression occur in response to pregnancy and the presence of conceptuses in utero. Studies of the porcine endometrial transcriptome revealed effects of pregnancy on both mRNA [20, 21] and microRNA (miRNA; [22–26]) populations. MicroRNAs are approximately 22 nucleotide RNAs that inhibit gene expression post-transcriptionally through mRNA destabilization/degradation and translational repression [27]. Thus, efforts to predict miRNA–mRNA interactions through paired expression profiling are important functionally.

Given documented [14], negative effects of lactocrine deficiency from birth on maternal capacity to produce large, viable litters in adulthood, it was hypothesized that suboptimal lactocrine support, reflected by minimal serum iCrit within 24 h of birth, would affect patterns of endometrial gene expression during the periattachment period of early pregnancy. Therefore, objectives of this study were to determine effects of lactocrine deficiency from birth on the porcine endometrial transcriptome in the same animals as adults, including predicted miRNA–mRNA interactions, on PxD 13.

Materials and methods

Animals and experimental design

Gilts (*Sus scrofa domesticus*) were born and raised from a herd of crossbred maternal line (Landrace and Yorkshire genetics) pigs at the U. S. Meat Animal Research Center (USMARC) in Clay Center, Nebraska. All procedures involving animals were reviewed and approved by the USMARC Institutional Animal Care and Use Committee and conducted in accordance with the Federation of Animal Science Societies (2010) guidelines for the care and use of agricultural animals in research.

Gilts and sows up to fourth parity were observed for estrous behavior and mated by artificial insemination using semen from maternal line boars from several commercial sources according to standard operating procedures at USMARC. On day 110 of gestation, dams were moved into farrowing crates and allowed to farrow naturally. If farrowing did not occur by day 116 of gestation, gilts were injected with Estrumate (1 ml; Intervet Merck Animal Health, Madison, NJ) to induce farrowing, which is standard operating procedure at USMARC. This procedure does not affect litter average iCrit [28].

The experimental design is illustrated in Figure 1. On the day of birth (PND 0), piglets were processed (ear notch, tail dock, needle teeth clipped, penicillin, and iron dextran injection) using standard operating procedures. Additionally, a jugular blood sample was collected from each gilt offspring within 24 h of birth. As described previously [15], clotted blood samples from each gilt were centrifuged at 1000 × g for 10 min. Equal amounts (50 μl) of serum and 40% (wt/vol) ammonium sulfate in distilled water were mixed and the precipitated sample was loaded into a hematocrit centrifuge tube. Samples were centrifuged at full speed (12,000 × g) for 10 min. The iCrit ratio was calculated by taking the length of the

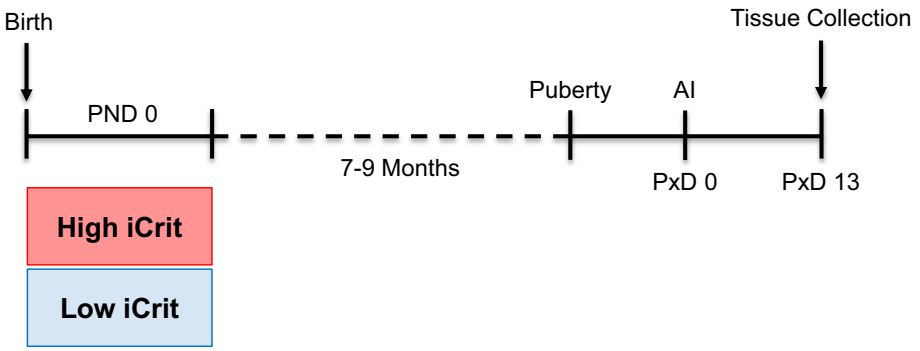

Figure 1. Experimental design. Within 24 h of birth (PND 0), jugular blood samples were collected from gilts, serum immunocrit (iCrit) ratios were measured, and these values were used to assign gilts to high or low iCrit groups. At puberty (7–9 months of age), following at least one estrous cycle of normal duration, gilts were bred by artificial insemination (AI) using up to two doses of single sire semen (pregnancy day = PxD 0). On PxD 13, high (n = 8), and low (n = 7) iCrit gilts were euthanized and tissues were collected as described in Materials and Methods section.

precipitate divided by the length of the diluted serum in the tube. Within each litter, gilts with an iCrit of 0.05 or lower (low iCrit; n = 8) were matched with a littermate of similar birth weight and an iCrit of greater than 0.10 (high iCrit; n = 8). Overall, serum iCrit was greater ($P < 0.001$) in high (0.115 ± 0.01) as compared to low (0.033 ± 0.01) iCrit groups. If litter size exceeded 12 piglets per litter, male piglets were cross-fostered to other litters if available, according to standard operating procedures at USMARC. Overall, neonatal gilts from approximately 300–400 litters were screened on their day of birth to determine iCrit status. Of these, paired adult littermates from a total of eight litters, defined as high or low iCrit at birth, were used in these PxD 13 studies.

On day 15 of age, all gilts received creep feed and were weaned on approximately day 24. At weaning, gilts were housed in the USMARC nursery for 4 weeks and fed the USMARC standard nursery ration. After 4 weeks, gilts were moved to finishing barns and fed standard USMARC grower and finisher diets. At 170 days of age, gilts were moved to the gilt breeding area and were observed daily for estrous behavior. Following at least one estrous cycle of normal duration (17–23 days), gilts were mated at subsequent estrus by artificial insemination using commercial maternal line semen, and mated again 24 h later if still in estrus. On day 13 of pregnancy (PxD 13), gilts were humanely slaughtered at the USMARC abattoir and reproductive tracts were collected. Corpora lutea were counted as an indicator of ovulation rate. Uteri were trimmed free of the broad ligament, and uterine lengths (cm) and wet weights (g) were recorded.

To confirm pregnancy and collect uterine flushings, a clamp was placed at the cervix and an incision was made in the uterus at the tip of the uterine horn near the uterotubal junction. Using a syringe and a blunt needle, 0.9% saline (20 ml) was injected into the uterine lumen from the posterior end of each uterine horn, and the saline bolus was massaged through the length of the uterus until it emerged from the incised end. The saline flushing from each uterine horn was collected into a 100-mm plastic petri dish, and each flushing was examined for the number of conceptuses present by observation of corresponding embryonic discs under a stereomicroscope (Nikon Instruments Inc., Melville, NY). After flushing, each uterine horn was opened longitudinally, and endometrial tissue was collected from approximately the middle of the horn. Endometrial samples were frozen in liquid nitrogen and stored at −80°C until total RNA was extracted. One low iCrit animal was not pregnant and removed from the study (final sample size: low iCrit, n = 7; high iCrit, n = 8).

Conceptuses were removed from each uterine luminal flushing (ULF), and the flushings from each gilt were combined and centrifuged (2100 × g for 20 min at 4°C). Aliquots of pooled ULF were then frozen at −80°C until analysis. Estradiol-17 beta concentrations were determined in ULF samples from each pregnant gilt using a commercially available ELISA (EIA-2693, DRG International, Inc.; Springfield, NJ). This assay was previously reported for use in swine [29] and validated by determining parallelism between the manufacturer's standard curve and serial dilutions of three ULF samples. The coefficient of variation between these curves was 15.4%. The dynamic range for the ELISA was between 9.714 and 2000 pg/ml for estradiol-17 beta. ULF samples were assayed in duplicate within one assay with an intra-assay coefficient of variation of 3.68%. Total ULF estradiol content was calculated by multiplying ULF estradiol concentration values for each gilt by values for corresponding ULF recovery volumes.

Data for number of corpora lutea, total uterine length and weight, conceptus number, and ULF estradiol content were analyzed statistically using General Linear Model procedures (SAS 2013, Cary, NC). Data were subjected to analyses of variance considering the main effect of PND 0 iCrit. Results are presented as least squares means ± standard error of the mean.

Endometrial RNA isolation and analysis

Total RNA (including miRNA and mRNA) was isolated from endometrial tissue (50 mg/uterine horn) for each sample using the miRNeasy Mini Kit (Qiagen Inc., Valencia, CA) following the manufacturer's protocol. RNA quantity was measured using a Qubit® 2.0 Fluorometer (Invitrogen, Carlsbad, CA), and RNA integrity was assessed using an Agilent 2100 Bioanalyzer (Applied Biosystems, Carlsbad, CA). Samples with an RNA integrity number ≥7.5 were used for library preparation for mRNA sequencing (mRNAseq) and miRNA sequencing (miRNAseq).

Preparation of mRNA and miRNA libraries

All mRNAseq and miRNAseq procedures were performed at the Genomic Services Laboratory, HudsonAlpha Institute for Biotechnology, as previously described [9, 10]. Briefly, total RNA (500 ng) from each endometrial sample was used for mRNA and miRNA library preparation. For mRNAseq, polyadenylated (polyA) RNAs were isolated using NEBNext Magnetic Oligo d(T)25 Beads (New England BioLabs, Inc.). After polyA selection, RNA was fragmented

and primed for first-strand synthesis using the NEBNext First Strand Synthesis Module, followed by second-strand synthesis using the NEBNext Second Strand Synthesis Module. Sample processing, including barcoding of individual samples, followed standard library preparation protocol using NEBNext DNA Library Prep Master Mix Set for Illumina with slight modifications, as previously described [10]. For miRNAseq, the NEBNext Small RNA Library Prep Set for Illumina (New England Biolabs Inc., Ipswich, MA) was followed according to the manufacturer's protocol.

mRNA and miRNA library quantities were assessed using a Qubit® 2.0 Fluorometer, and library quality was determined using a DNA High Sense chip on Agilent 2100 Bioanalyzer. Further library quantification was completed using the qPCR-based KAPA Biosystem Library Quantification kit (Kapa Biosystems Inc., Woburn, MA). For mRNAseq, each library was diluted to a final concentration of 12.5 nM. For miRNAseq, individual sample libraries were diluted to a final concentration of 1.25 nM. Equimolar amounts of individual barcoded samples from each group were pooled prior to sequencing.

mRNA and miRNA sequencing and data analysis

Paired-end mRNAseq, at over 25 million reads per individual barcoded sample, was performed using a HiSeq 2500 (Illumina, Inc., San Diego, CA) following the manufacturer's protocol and as previously described [10]. Summary of mRNAseq alignment statistics is shown in Supplemental Table S1. Reads were mapped to the *Sus scrofa* 11.1 build of the porcine genome (GenBank Assembly Accession: GCA_000003025.6; National Center for Biotechnology Information [NCBI]) using Avadis NGS (version 3.1.1; Strand Scientifics, CA). Alignment and filtering of mapped reads were conducted as previously described [10]. Samples were grouped according to their respective identifiers. Normalized gene expression was quantified using the trimmed mean of M-values method [30]. Human orthologs of unannotated differentially expressed genes were identified using the Reciprocal Best Hits method [31], whereby genes g_1 and g_2 in the pig and human genome, respectively, are deemed orthologs if g_2 is the best hit when g_1 is queried in a BLAST search against the database of human genes and g_1 is the best hit when g_2 is queried in a BLAST search against the database of pig genes.

miRNAseq was conducted using an Illumina HiSeq 2500 instrument (Illumina Inc.) at 50-bp single-end condition generating approximately 15 million reads per sample. Quality control checks, adapter trimming, and read filtering were performed as previously described [9]. Filtered reads were used to extract and count miRNAs which were annotated with miRBase release 21 database [32–36]. Samples were grouped according to their respective identifiers followed by quantification of miRNA abundance [30].

Differentially expressed mRNAs and miRNAs, based on fold change ($\geq \pm 1.5$), were identified with respect to neonatal iCrit (high iCrit versus low iCrit). Probability values for each differentially expressed mRNA and miRNA were estimated by z-score calculations along with a Benjamini-Hochberg false discovery rate of ≥ 0.05. Data were subjected to principal component analysis using Avadis NGS (version 3.1.1; Strand Scientifics, CA). Relative fold change in mRNA abundance was illustrated using volcano plots generated for each comparison using R Programming (GNU General Public License; www.r-project.org).

For mRNAseq data, gene enrichment analyses were performed using Database for Annotation, Visualization, and Integrated Discovery (DAVID; version 6.8) [37, 38] and Protein Analysis Through Evolutionary Relationships (PANTHER; version 13.0) [39]. Ingenuity Pathway Analysis (IPA) software (Qiagen Redwood City, CA; www.qiagen.com/ingenuity) was used for functional annotation and related biological pathway analyses. Relationships between differentially expressed miRNAs and their respective differentially expressed mRNA targets were determined using Qiagen's Ingenuity Pathway Analysis MicroRNA Target Filter (IPA, Qiagen Redwood City; www.qiagen.com/ingenuity). By applying Qiagen's IPA expression pairing tool, miRNA–mRNA pairings were limited to canonical relationships, defined by inverse associations between miRNAs and their target mRNAs.

Quantitative real-time polymerase chain reaction

Validation of mRNAseq data was done by quantitative real-time polymerase chain reaction (qPCR) using the same RNA used to generate cDNA libraries. Endometrial RNA from individual pigs in each group was pooled to create high and low iCrit samples for qPCR, with the specific objective to provide technical validation for mRNAseq. Reverse transcription (2 μg/sample) was performed on a Peltier Thermal Cycler-200 (Bio-Rad Laboratories, Inc.) using the SuperScript III First-Strand Synthesis System (Life Technologies). Quantitative RT-PCR (50 ng/sample) was conducted using SYBR Green and universal thermal cycling parameters (40 cycles), as indicated by the manufacturer on a StepOne Plus System (Applied Biosystems/Life Technologies).

Primers were designed using Primer Quest software (Integrated DNA Technologies, Inc.) and synthesized by Sigma-Aldrich. Primer sequences (Supplemental Table S2), directed to the porcine genome, were evaluated for quality by amplifying serial dilutions of the cDNA template. To ensure specific amplification, control qPCR reactions included substitution of water only, in place of primers and template. Dissociation curves for primer sets were assessed to ensure that no amplicon-dependent amplification occurred.

Nine endometrial genes chosen for qPCR validation included those for which relative expression, determined by RNAseq, increased or decreased more than 1.5-fold, or were unchanged in high as compared to low iCrit gilts on PxD 13. These genes included serum amyloid A 3 (*SAA3*), solute carrier family 5 member 1 (*SLC5A1*), S100 calcium-binding protein A12 (*S100A12*), mucin 4 (*MUC4*), retinol binding protein 4 (*RBP4*), secreted phosphoprotein 1 (*SPP1*), fibroblast growth factor 7 (*FGF7*), leukemia inhibitory factor (*LIF*), and solute carrier family 24 member 4 (*SLC24A4*). Porcine cyclophilin A (*PPIA*) was constitutively expressed between low and high iCrit samples (data not shown) and was therefore used for normalization as the endogenous reference gene [40]. Data generated by qPCR were analyzed using the $\Delta\Delta$CT method as described by Applied Biosystems (ABI User Bulletin 2, 2001). Pearson correlation coefficient was determined to compare mRNA expression fold-change results obtained by mRNAseq and qPCR.

Results

Effects of lactocrine deficiency on ovarian and uterine endpoints and endometrial mRNA expression on PxD 13

When high and low iCrit gilts were compared on PxD 13, no differences in corpora lutea number (16.4 ± 1 vs 14.6 ± 1 CL), uterine length (128.7 ± 8.5 vs 131.0 ± 7.9 cm), uterine wet weights (890.8 ± 55.1 vs 828.4 ± 58.9 g), conceptus recovery (7.6 ± 1 vs 6.4 ± 1 conceptuses), or total recoverable ULF estradiol content

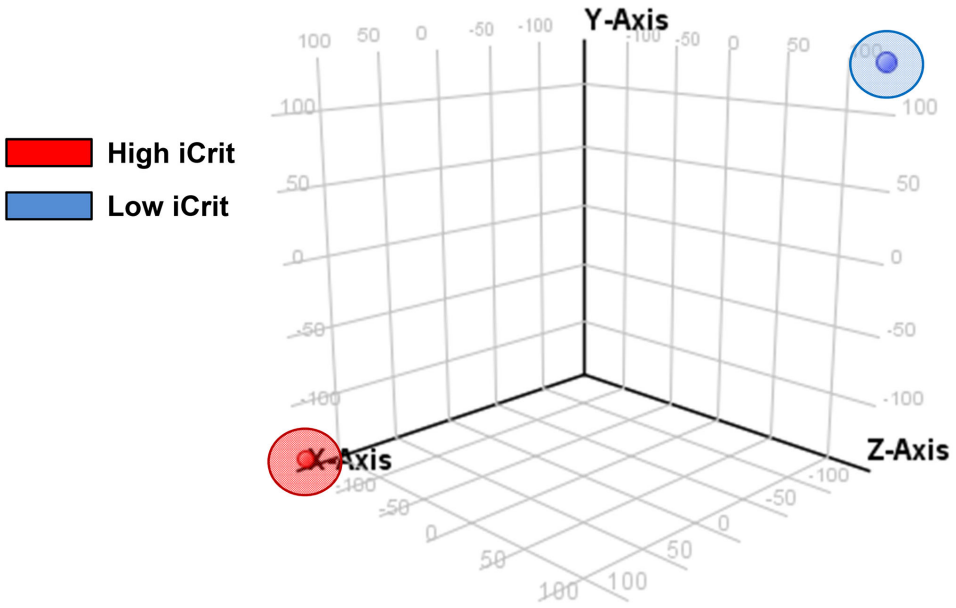

Figure 2. Principal component analysis (PCA) plot of mRNAseq data. PCA plot of pooled porcine endometrial samples on PxD 13 showing the mean of expressed mRNAs for high iCrit ((red/lower left) and low iCrit (blue/top right) samples.

(9.5 ± 4.7 vs 12.3 ± 5.1 ng) were observed. Endometrial mRNA data at PxD 13 for high and low iCrit groups clustered separately according to principal component analysis (Figure 2). Effects of lactocrine deficiency at birth, as reflected by serum iCrit, on endometrial gene expression at PxD 13 are illustrated in Figure 3A. Out of 28,224 protein coding mRNAs identified in the *Sus scrofa* 11.1 database, 1157 mRNAs were differentially expressed (≥1.5-fold, $P < 0.05$) in high as compared to low iCrit gilts on PxD 13 (Figure 3A, Supplemental Table S3). Of these differentially expressed mRNAs, 562 decreased and 595 increased in the endometrium of high versus low iCrit gilts (Figure 3A, Supplemental Table S3). The top 10 most highly differentially expressed endometrial mRNAs in high as compared to low iCrit gilts on PxD 13 included *NPY, ACOD1, CTRL, TGM3, TNIP3, FAM151A, CRISP3, NLRC4, FGA,* and *ACSBG1* (Supplemental Table S3).

Results of technical validation of mRNAseq data by qPCR are shown in Figure 3B. Expression of nine transcripts including *SAA3, SLC5A1, S100A12, MUC4, RBP4, SPP1, FGF7, LIF,* and *SLC24A4* was evaluated. A positive correlation between mRNAseq and qPCR data was identified ($r = 0.91$, $P < 0.001$).

Gene enrichment analyses of differentially expressed mRNAs

Differentially expressed endometrial mRNAs in high as compared to low iCrit gilts on PxD 13 were categorized by enriched biological processes and pathways using DAVID, Reactome, IPA, and PANTHER (Figures 4 and 5). The top 10 significantly enriched gene ontology (GO) terms identified by DAVID functional annotation analysis included multiple terms related to immune response, such as "defense response," "response to external stimulus," "regulation of leukocyte migration," and "inflammatory response" (Figure 4A). Other enriched GO terms identified by DAVID included "ion transport," "nitrogen compound transport," "reproduction," and "reproductive process."

Figure 4B illustrates enriched biological pathways within the differentially expressed mRNA dataset as identified by Reactome. Pathways affected by neonatal immunocrit on PxD 13 in the endometrium included those related to ECM remodeling, such as "collagen degradation," "activation of matrix metalloproteinases," "molecules associated with elastic fibres," and "degradation of the extracellular matrix." Other enriched pathways included "G alpha (i) signaling events," "peptide ligand-binding receptors," "chemokine receptors bind chemokines," "O-linked glycosylation of mucins," and "ligand-gated ion channel transport."

Functional annotation categories identified by IPA for differentially expressed mRNAs in the endometrium of high versus low iCrit gilts on PxD 13, selected based upon their association with biological processes related to uterine development, structure, and function, are shown in Figure 4C. Predominant terms specific to differential endometrial mRNA expression were related to cellular function and development. With regard to cellular function, enriched categories included "cell-to-cell signaling and interaction," "cellular function and maintenance," "cellular movement," "immune cell trafficking," and "cellular growth and proliferation." Enriched developmentally-related categories included "tissue morphology," "endocrine and reproductive system development and function," and "embryonic and organismal development."

Figure 5 illustrates enriched GO biological processes for differentially expressed mRNAs on PxD 13 as identified by PANTHER. Processes sensitive to lactocrine deficiency included "cellular process," "reproduction," "biological regulation and adhesion," "response to stimulus," as well as "developmental, metabolic, and immune system" processes. Across analyses, overall top enriched biological processes on PxD 13 were related to immune response, ECM remodeling, cell function, and reproduction/development.

Selected differentially expressed endometrial mRNAs

Selected differentially expressed mRNAs with known or postulated roles in implantation are presented in Table 1. The gene family

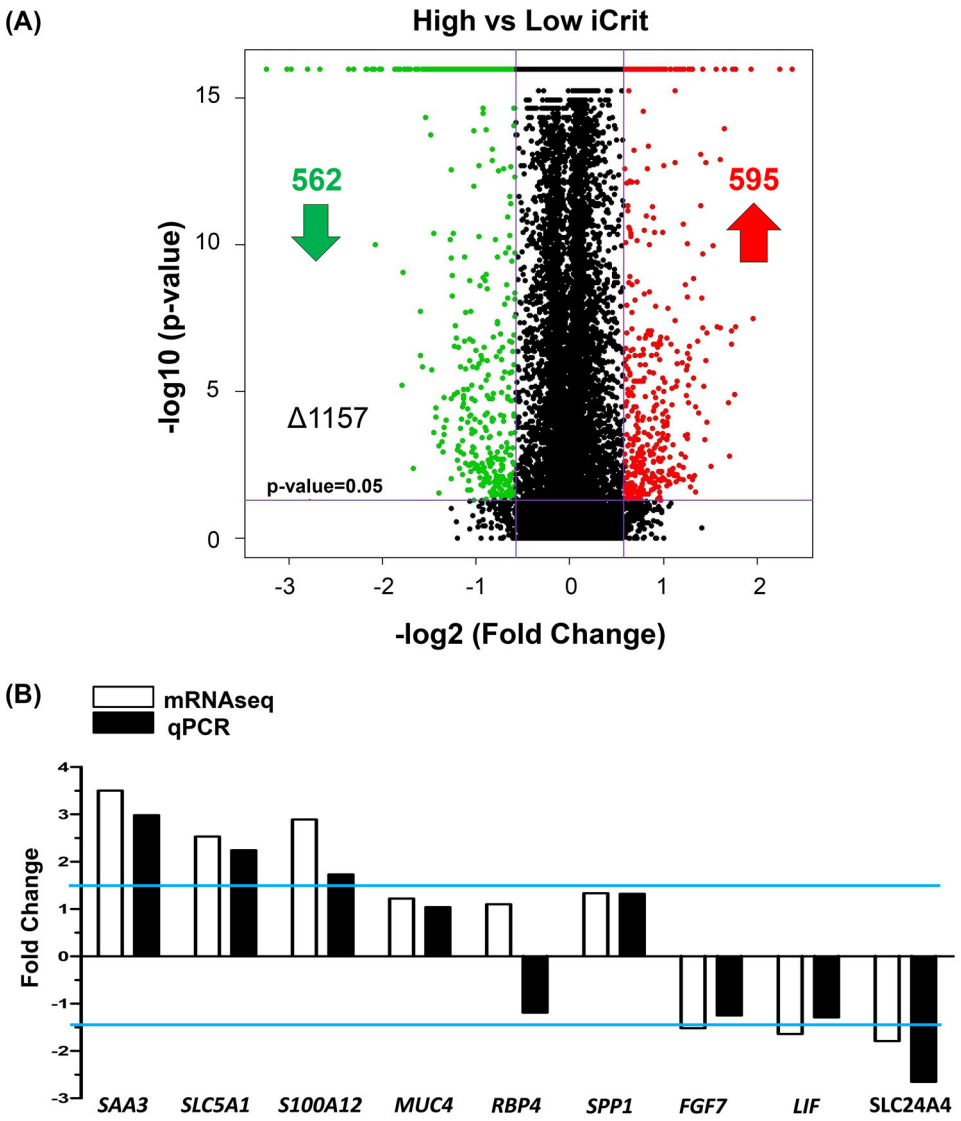

Figure 3. (A) Volcano plot demonstrating differences in endometrial expression of mRNAs on PxD 13 in high versus low iCrit gilts. Increased expression is indicated in red/up arrow/dark gray and decreased expression in green/down arrow/light gray (fold-change ≥ 1.5). Black indicates mRNA expression that did not differ between groups. The horizontal line indicates $P = 0.05$. The total number of differentially expressed mRNAs is given (Δ value). The number of mRNAs for which expression was decreased (down arrow) or increased (up arrow) is shown. (B) Results of qPCR validation for nine mRNAs identified by mRNAseq for high versus low iCrit groups. White bars indicate mRNAseq-based fold change; black bars indicate qPCR-based fold change. Horizontal lines indicate 1.5-fold change (+/–). A positive correlation between mRNAseq and qPCR results was observed ($r = 0.91$, $P < 0.001$).

with the most abundant, lactocrine-sensitive elements involved solute carrier (SLC) membrane transporters. For this group, relative expression of 20 SLC transcripts increased and 18 decreased in the endometrium of high as compared to low iCrit gilts (Supplemental Table S3). Other lactocrine-sensitive, differentially expressed endometrial transcripts included those involved in prostaglandin signaling (*AKR1B1*, *PTGS1*, and *SLCO2A1*), immune response (*S100A8, CXCL10, LIF, IL1A*, and *ITGAM*), and endometrial receptivity (*ACOD1, STC1, LPAR3, DKK1*, and *BMP2*). Additionally, a number of endometrial transcripts related to uterine remodeling and proteolysis were lactocrine sensitive. These included matrix metalloproteinases (*MMP12, MMP7, MMP8*, and *MMP13*), mucins (*MUC20, MUC6*, and *MUC13*), ADAMs (a disintegrin and metalloproteinase; *ADAM23, ADAM2, ADAM7*, and *ADAMTS19*), and keratin 23 (*KRT23*; Table 1). With regard to the keratin (KRT) gene family, expression of eight transcripts (*KRT79, KRT14, KRT20, KRT23, KRT35, KRT5, KRT36*, and *KRT80*) increased, and one transcript (*KRT6A*) decreased in the endometrium of high as compared to low iCrit gilts (Supplemental Table S3).

Effects of lactocrine deficiency on endometrial miRNA expression on PxD 13

From 461 mature miRNAs identified in the porcine miRBase release 21, 6 miRNAs were differentially expressed (≥1.5-fold, $P < 0.05$) in the endometrium of high versus low iCrit gilts on PxD 13.

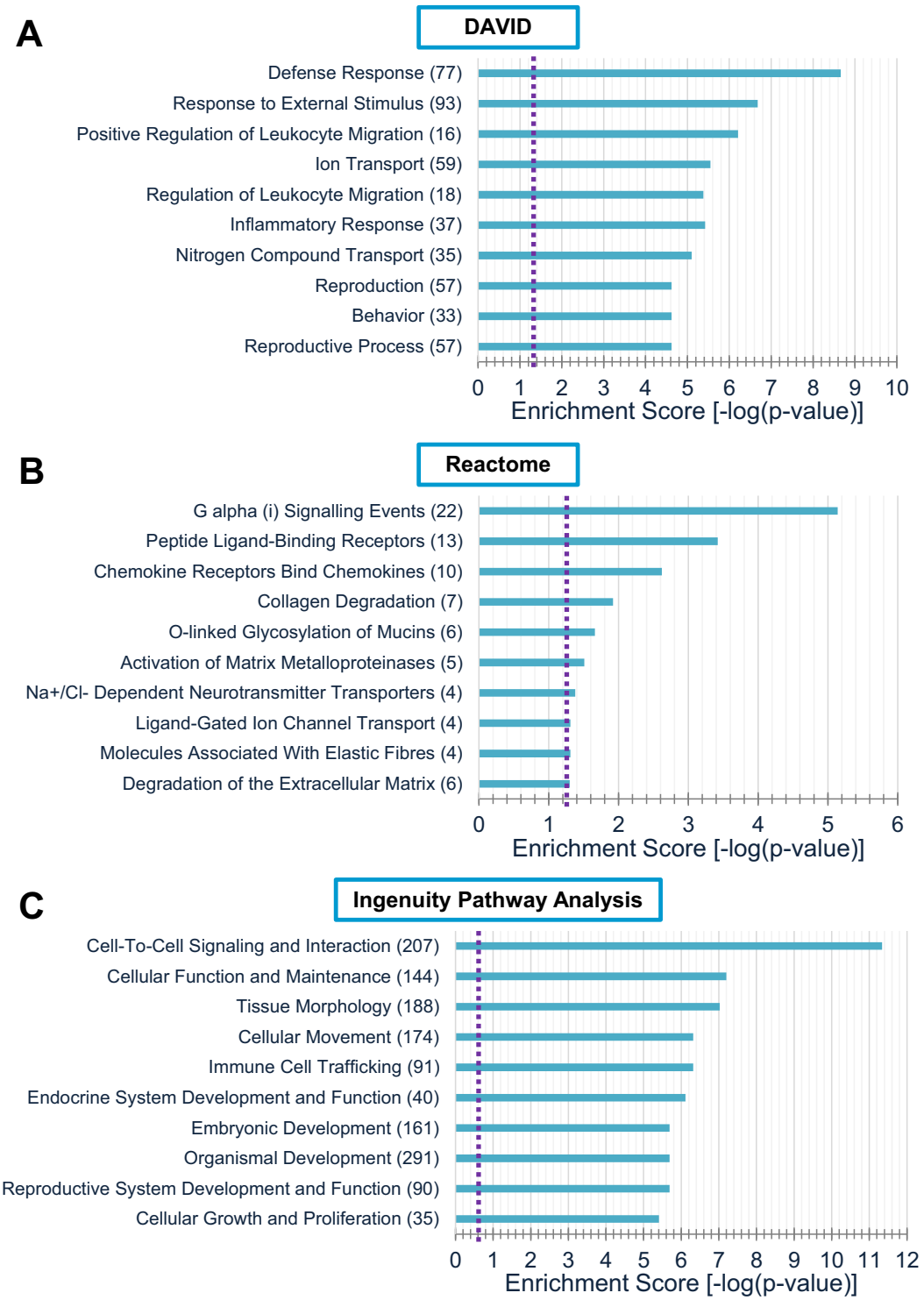

Figure 4. Selected functional annotation categories for differentially expressed endometrial mRNAs in high versus low iCrit gilts on PxD 13 as identified by (A) DAVID, (B) Reactome, and (C) IPA. Values within parentheses indicate the number of annotated mRNAs that are involved in the corresponding functional term. Enrichment scores were calculated by taking the geometric mean of the *P*-values associated with differentially expressed transcripts (in $-\log_{10}$ scale). Dashed vertical line indicates $P = 0.05$.

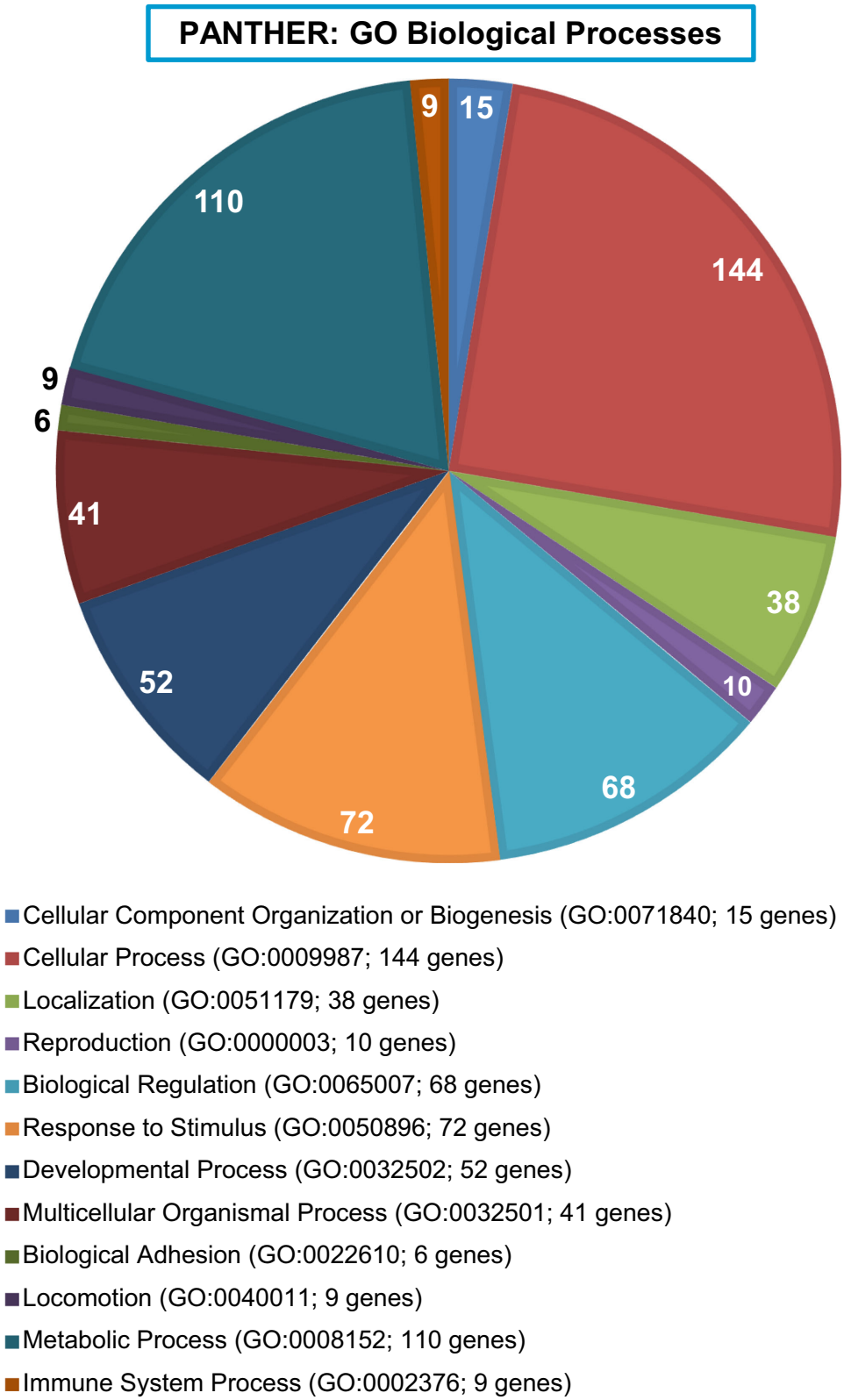

Figure 5. Gene ontology (GO) of biological processes for differentially expressed endometrial mRNAs in high versus low iCrit gilts on PxD 13 as classified by PANTHER. A total of 325 differentially expressed genes were identified by PANTHER and classified according to their GO. The numbers on the pie chart represent the number of genes within the GO category. GO identification numbers are shown in parentheses. For orientation, the list begins with Cellular Component Organization or Biogenesis associated with 15 differentially expressed genes and proceeds clockwise.

Differentially expressed miRNAs included miR-129a-3p, miR-7135–5p, miR-371–5p, miR-338, miR-365–5p, and miR-144 (listed in descending order in Table 2). Of those, five of the porcine miRNAs identified had human orthologs. No differential miRNA expression events greater than twofold were identified.

Integrated target prediction analyses

The workflow and output for miRNA–mRNA data integration and bioinformatic analyses are illustrated in Figure 6. Procedures enabled integration of data for 1157 mRNAs and 6 miRNAs determined to be differentially expressed by endometrium obtained from high and low iCrit gilts on PxD 13. Relationships between differentially expressed miRNAs and respective mRNA targets were limited to inverse pairings (i.e. expression of miRNA increased and mRNA targets decreased) and those transcripts with human orthologs identified by IPA. Thus, a total of five differentially expressed miRNAs were predicted to target 62 differentially expressed mRNAs (Figure 6). Table 3 lists the five differentially expressed miRNAs and predicted differentially expressed mRNA targets as identified by IPA. Additional information regarding differentially expressed mRNA targets for each miRNA is presented in Supplemental Table S4. Illustration of predicted miRNA–mRNA interactions is presented as an interactome network in Figure 7. Only inverse relationships are presented, where endometrial expression of miRNAs increased and expression of associated mRNA targets decreased between high and low iCrit gilts on PxD 13. Increased expression of transcripts in high as compared to low iCrit gilts is shown in red/dark gray, and decreased expression is shown in green/light gray. Note, several differentially expressed mRNAs are targeted by more than one miRNA. Further, interactions between mRNA transcripts are also presented.

Enriched biological processes associated with endometrial mRNAs targeted by miRNAs between high and low iCrit gilts on PxD 13 as identified by DAVID are listed in Table 4. MicroRNA–mRNA interactions were predicted to be involved with similar processes observed for mRNAseq data alone, including those related to development and regulation of cellular functions, such as cell motility. Due to the limited number of predicted miRNA–mRNA interactions, enriched biological processes were not observed for Reactome and PANTHER analyses of mRNA targets.

Discussion

The lactocrine hypothesis for maternal programming of uterine development posits that disruption of lactocrine signaling from birth can alter the neonatal uterine developmental program and trajectory with long-term consequences for reproductive performance in adults [41]. Consistently, data for neonates showed that imposition of a lactocrine-null condition from birth, by milk replacer-feeding, altered patterns of porcine uterine wall development and global patterns of uterine gene expression by PND 2 [9–11] with overt, negative effects on endometrial histogenesis by PND 14 [11]. Likewise, lactocrine deficiency from birth, reflected by low serum iCrit within 24 h of birth, inhibited uterine wall development by PND 14 [8], as reflected by reduced endometrial gland genesis and immunostaining for proliferating cell nuclear antigen. Further, in a study involving 799 female pigs followed over four parities, lactocrine deficiency from birth was associated with reduced average preweaning growth rate, increased age at puberty, and, critically, reduced live litter size with no effect of parity [14]. Present data support the idea that permanent impairment of reproductive performance in lactocrine-deficient, adult female pigs is associated with alterations in endometrial function, reflected by differential endometrial gene expression patterns between high and low iCrit gilts during the periattachment period of early pregnancy. Results establish a long-term effect of neonatal lactocrine programming on adult endometrial function in the pig.

Establishment and maintenance of an embryotrophic uterine environment require that the adult, periattachment stage endometrium integrates systemic signals of maternal, as well as local signals of conceptus origin [19]. Results indicating that lactocrine deficiency from birth did not affect uterine horn length or wet weight, number of corpora lutea, number of conceptuses, or total recoverable ULF estradiol content, provide support for the idea that lactocrine deficiency did not affect adult uterine morphology, and that systemic and local signals driving endometrial function were similar in low and high iCrit gilts on PxD 13. Evidence of differential gene expression patterns between these groups likely reflects differences in the capacity of these endometrial tissues to integrate maternal and conceptus signals as necessary to insure development of an optimally embryotrophic uterine environment.

Lactocrine deficiency from birth had substantial effects on patterns of endometrial gene expression, as defined by the transcriptome in adult gilts on PxD 13. Results enabled definition of the size (number of affected transcripts), directionality (increased and decreased expression), and, to the extent that the porcine genome is annotated [42], identification of individual transcriptomic elements of the endometrial domain of response associated with lactocrine disruption of the neonatal uterine developmental program [7–10]. Elements of this response domain are, by definition, lactocrine sensitive. Subdomains of response, defined by biological processes identified using DAVID, Reactome, IPA, and PANTHER, included some that were similar to those described for the adult porcine endometrium in response to pregnancy on days 12 and 14 [20, 21]. Examples included defense response, proteolysis, and cell adhesion. Elements of the adult endometrial, lactocrine-sensitive transcriptome not grouped into subdomains informatically, but that could affect endometrial functionality and conceptus–endometrial interactions during the periattachment period, were also defined as discussed below.

Genes involved in epithelial cell transport mechanisms

During pregnancy, uterine epithelial secretory products, as well as factors delivered to the uterine lumen from maternal plasma, support conceptus development and implantation [43]. Components of uterine luminal fluid, including glucose, fructose, and amino acids [44], require specific epithelial transporter proteins to facilitate their movement across cellular compartments and into the uterine lumen [45]. One such class of mammalian transporters is the SLC superfamily. Members of this superfamily were implicated in porcine placental function [45–47]. In the present study, several differentially expressed SLC transcripts were identified in the endometrium of high as compared to low iCrit gilts. Included were sodium-dependent glucose transporters *SLC5A1* and *SLC5A9*, as well as glucose-activated sodium channel *SLC5A4* and short-chain fatty acid transporter *SLC5A8* [48], for which expression was greater in high iCrit gilts. Estrogen-sensitive expression of *SLC5A1* was documented for porcine endometrial luminal epithelium on PxD 12–13 [47]. This suggested that locally produced, conceptus-derived estrogens induce endometrial expression of this glucose transporter. Glucose is transported passively from maternal blood into the uterine lumen through a process facilitated by conversion to fructose in the placenta [49], as necessary for porcine conceptus survival.

Table 1. Selected differentially expressed endometrial mRNAs in high versus low iCrit gilts on PxD 13 with known or postulated roles in implantation.

Functional category	Entrez ID	Gene ID	FC	Gene name
Epithelial cell transport mechanisms	397113	*SLC5A1*	2.53	Solute carrier family 5 member 1
	100522082	*SLC5A9*	2.35	Solute carrier family 5 member 9
	397376	*SLC5A4*	1.9	Solute carrier family 5 member 4
	100524807	*SLC5A8*	1.72	Solute carrier family 5 member 8
Prostaglandin synthesis and secretion	396816	*AKR1B1*	2.5	Aldo-keto reductase family 1 member B
	397541	*PTGS1*	1.77	Prostaglandin G/H synthase 1
	100144510	*SLCO2A1*	−1.5	SC organic anion transporter member 2A1
Immune response	100127488	*S100A8*	2.84	S 100 calcium binding protein A8
	494019	*CXCL10*	2.66	C-X-C motif chemokine 10
	399503	*LIF*	−1.64	Leukemia inhibiting factor
	397094	*IL1A*	−1.76	Interleukin 1 alpha
	397459	*ITGAM*	−1.80	Integrin alpha M
Endometrial receptivity	100524951	*ACOD1*	8.09	Aconitate decarboxylase 1
	100134954	*MUC20*	2.82	Mucin 20, cell associated
	100125345	*STC1*	2.29	Stanniocalcin 1
	100626121	*MUC6*	1.95	Mucin 6, Oligomeric Mucus/Gel-Forming
	100125829	*MUC13*	1.68	Mucin 13, Cell Surface Associated
	100113360	*LPAR3*	1.64	Lysophosphatidic acid receptor 3
	100157640	*DKK1*	−1.66	Dickkopf-related protein 1
	100157103	*BMP2*	−1.72	Bone morphogenetic protein 2
Implantation-related uterine remodeling and proteolysis	100101475	*MMP12*	4.09	Matrix metalloproteinase 12
	397411	*MMP7*	2.57	Matrix metalloproteinase 7
	100519795	*KRT23*	2.4	Keratin 23
	100523811	*MMP8*	2.07	Matrix metalloproteinase 8
	397346	*MMP13*	1.58	Matrix metalloproteinase 13
	100518044	*ADAM23*	−1.55	A disintegrin and metalloprotease domain 23
	397006	*ADAM2*	−1.57	A disintegrin and metalloprotease domain 2
	100518181	*ADAMTS19*	−1.63	ADAM metallopeptidase with thrombospondin type 1 motif 19
	100156770	*ADAM7*	−1.64	A disintegrin and metalloprotease domain 7

Table 2. Differentially expressed endometrial miRNAs in high versus low iCrit gilts on PxD 13.

Gene ID	Swine miRNA Name	Swine miRBase ID[1]	Human miRNA Name	Human miRBase ID[1]	FC High iCrit vs Low iCrit
MI0023568;_1	ssc-miR-7135-5p	MIMAT0028145	No ortholog	No ortholog	1.92
MI0014773;_1	ssc-miR-338	MIMAT0015713	hsa-miR-338-3p	MIMAT0000763	1.89
MI0013120;_2	ssc-miR-365-5p	MIMAT0017376	hsa-miR-365b-5p	MIMAT0022833	1.81
MI0031640;_1	ssc-miR-371-5p	MIMAT0037081	hsa-miR-371b-3p	MIMAT0019893	1.67
MI0022132;_1	ssc-miR-144	MIMAT0025364	hsa-miR-144-3p	MIMAT0000436	1.64
MI0013169;_1	ssc-miR-129a-3p	MIMAT0013959	hsa-miR-129-2-3p	MIMAT0004605	1.51

[1]Mature miRNA ID.

Fructose is also present in porcine uterine luminal fluids during early pregnancy, and uterine luminal fluid fructose concentrations increase between PxD 11 and 15 [46]. Fructose is produced when glucose is reduced to sorbitol through the polyol pathway via the action of enzymes AKR1B1 and SORD. Porcine endometrial expression of both enzymes was documented for uterine luminal epithelium from PxD 13–17 [46]. Here, endometrial *AKR1B1* expression increased in high as compared to low iCrit gilts on PxD 13, while *SORD* was expressed consistently in both groups. Collectively, data can be interpreted to suggest that lactocrine deficiency from birth could affect porcine endometrial glucose transport and metabolism during the periattachment period of early pregnancy.

Genes involved in prostaglandin synthesis and secretion

The enzyme AKR1B1 also acts as a prostaglandin F synthase [50]. Expression of *AKR1B1* by porcine endometrial explants increased in response to conceptus secretory products including estrogens and IL1B, while treatment with an inhibitor of AKR1B1 activity decreased PGF2α production ex vivo [50]. This supports a role for AKR1B1 in endometrial production of PGF2α and events associated with maternal recognition of pregnancy in the pig [51]. Increased endometrial expression of *PTGS1*, an enzyme involved in prostaglandin E2 and F2α synthesis [50], was also observed in high iCrit gilts on PxD 13. Further, endometrial expression of the prostaglandin transporter *SLCO2A1* differed between high and low iCrit gilts. Implicated in regulation of uterine luminal prostaglandin influx during maternal recognition of pregnancy in the pig, SLCO2A1 expression was localized to basolateral membranes of uterine luminal epithelium and blood vessels during pregnancy [52]. Thus, lactocrine disruption of neonatal uterine development may affect patterns of adult endometrial prostaglandin biosynthesis and secretory dynamics during early pregnancy.

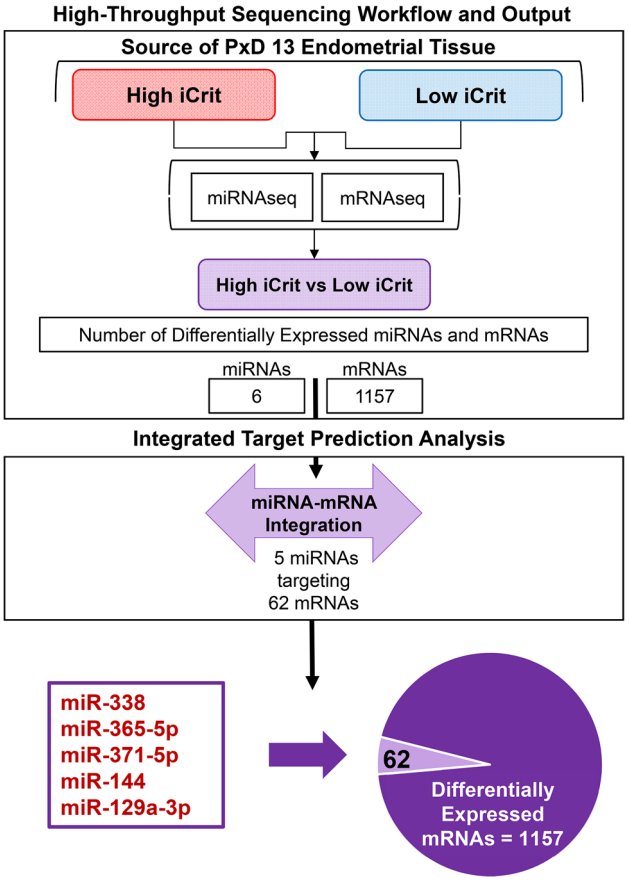

Figure 6. High-throughput sequencing workflow and output. Endometrial tissues were obtained from high and low iCrit gilts on PxD 13. Total endometrial RNA was isolated, and both mRNAs and miRNAs were sequenced as described in Materials and Methods section. Integrated target prediction analysis was conducted using IPA as described in Materials and Methods section. The numbers and names of differentially expressed miRNAs targeting differentially expressed mRNAs are presented.

Genes related to immune response

Mammalian implantation was described as an inflammatory process, involving immune responses required for conceptus survival [53]. Results of pathway analyses indicated that immunological processes associated with implantation were lactocrine sensitive. Some of these included regulation of leukocyte migration, immune cell trafficking, and immune system processes. Specific endometrial transcripts for which expression increased in high as compared to low iCrit gilts on PxD 13 included *S100A8*. A calcium binding protein S100A8 was implicated in regulation of endometrial inflammatory response to infection in post-partum cows [54], and increased in the porcine endometrium on PxD 12 [26]. Another lactocrine-sensitive element of the endometrial transcriptome *CXCL10* was implicated in immune cell recruitment to the endometrium during implantation in pigs [55]. Other mediators of immune function associated with the periattachment period [20, 21, 56] for which expression differed between high and low iCrit gilts included *LIF*, *IL1A*, and *ITGAM*. Porcine endometrial expression of *LIF* was reported from PxD 12–18 and LIF protein content in ULFs peaked on PxD 12 [57]. In mice, endometrial glandular LIF expression is required for implantation [58] and stimulates uterine luminal epithelial secretion of IL1A and prostaglandin E synthase during the peri-implantation period of pregnancy [56].

Genes related to endometrial receptivity

In the pig, one marker of endometrial receptivity to conceptus signals and implantation is down-regulation of progesterone receptor expression in luminal and glandular epithelium [59]. The associated up-regulation of ESR1 expression enables endometrial responsiveness to conceptus estrogens starting on PxD 12 [60]. In turn, conceptus estrogens stimulate transcription of genes identified here to be lactocrine-sensitive, including *AKR1B1* [50], *LPAR3* [61], and *STC1* [62], the products of which can affect cell growth and adhesion, solute transport, and dynamics of prostaglandin synthesis and secretion. Other lactocrine-sensitive transcripts include *ACOD1* (also known as *IRG1*; [63]), *DKK1* [64], and *BMP2* [65], all documented to mediate uterine receptivity and implantation in mice.

Factors affecting endometrial mucin expression and distribution are central to development of a receptive endometrium [66]. Here, endometrial expression of several mucin transcripts was determined to be lactocrine-sensitive. Included were *MUC20*, *MUC6*, and *MUC13*, not identified previously as products of the porcine endometrium. Mucins, which can be secreted (including MUC2 and MUC6) or transmembrane in nature (including MUC1, MUC4, MUC13, and MUC20), function to protect and stabilize epithelia [67, 68]. Transmembrane MUC13 was localized to the apical surface of rat uterine luminal epithelium during implantation, where it was suggested to facilitate blastocyst attachment [69]. Similarly,

Table 3. Integrated target prediction analysis[a] for differentially expressed endometrial miRNAs and mRNA targets in high versus low iCrit gilts on PxD 13 identified by Ingenuity Pathway Analysis.

miRNA	Number of targeted mRNAs[b]	Differentially expressed target mRNAs
miR-129a-3p	17	*LY6G6C, XKR4, KCNB1, MCF2, S100Z, TMEM257, AKAP5, SLC24A2, CPAMD8, PARD6B, SACS, MARCH1, BLOC1S6, PRKAR2A, KL, VNN2, KIAA1644*
miR-371-5p	16	*DUOXA2, HEPHL1, GABBR2, ANXA10, C7, HSD17B13, GDF11, ARNT2, MBL2, SCN4B, FAM131B, KL, RECK, CLOCK, INHBE, GPR173*
miR-365-5p	14	*CCND2, GREM1, FAM198A, CBY3, TGFBI, DQX1, BOLL, TREM2, RAB26, DMC1, KLK10, OMP, PLCH2, PRKAR2A*
miR-338	11	*DUOXA1, SCN1A, SLC26A7, FAM196B, DMRT2, ASTN2, TMEM196, FAM131B, SCAI, RAD54B, CHL1*
miR-144	9	*EYA1, CPS1, CCDC36, TMEM257, GALNT5, HIST2H4B, KIAA1024L, RAD54B, HEATR4*

[a]For cases where miRNA expression is decreased and mRNA expression is increased, or miRNA expression is increased and mRNA expression is decreased.
[b]Individual miRNAs can target multiple, overlapping populations of mRNAs.

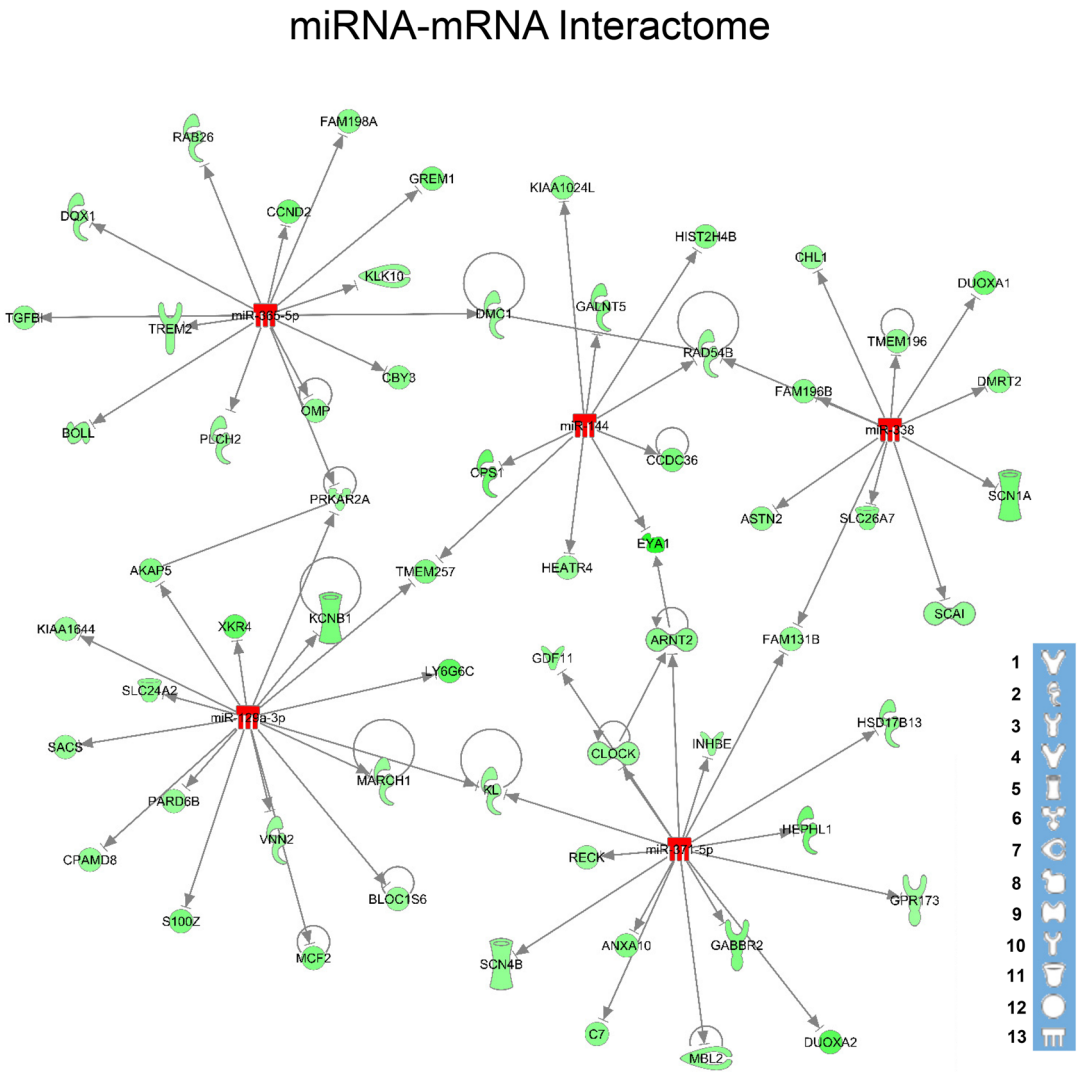

Figure 7. Integrated miRNA–mRNA interactome illustrating effects of high versus low iCrit on endometrial transcript interactions on PxD 13. Canonical, inverse miRNA–mRNA relationships are shown. Red/dark gray denotes increased and green/light gray denotes decreased transcript expression ($P < 0.05$). Color intensity indicates degree of change. IPA legend key (bottom right): (1) cytokine/growth factor; (2) enzyme; (3) G-protein coupled receptor; (4) growth factor; (5) ion channel; (6) kinase; (7) peptidase; (8) phosphatase; (9) transcription regulator; (10) transmembrane receptor; (11) transporter; (12) other; and (13) mature miRNA. For a complete list of all predicted miRNA–mRNA interactions, see Table 3.

endometrial *MUC13* expression increased during the period associated with conceptus elongation in cattle [70]. Both MUC1 [71] and MUC4 [72], not identified to be lactocrine-sensitive, regulate conceptus invasiveness and affect uterine epithelial receptivity to conceptus interactions in the pig.

Genes involved in implantation-related uterine remodeling and proteolysis

Matrix metalloproteinases (MMPs) function in extracellular matrix remodeling, and are required for successful implantation during pregnancy [73]. Differential endometrial expression of *MMP7*, *MMP8*, *MMP12*, and *MMP13* was identified between high and low iCrit gilts on PxD 13. In the pig, increased endometrial expression of *MMP7*, *MMP12*, and *MMP13* was associated with early pregnancy on day 12 [21]. Another category of metalloproteinases found to be lactocrine sensitive included members of the ADAM gene family (*ADAM23*, *ADAM2*, *ADAM7*, and *ADAMTS19*). ADAM family gene products function in cell-cell adhesion, cellular signaling, and cleavage of transmembrane cell-surface proteins [74], all processes associated with conceptus–endometrial interactions during the periattachment period [66]. Disregulation of endometrial mucin and metalloproteinase expression could be expected to affect adult reproductive performance as predicted by the lactocrine hypothesis [8].

Evidence presented here for porcine endometrial expression of keratin gene transcripts *KRT79*, *KRT14*, *KRT20*, *KRT35*, *KRT5*, *KRT36*, and *KRT80* is novel. Moreover, expression profiles for all of these transcripts reflected lactocrine programming effects on PxD 13. While specific functions of endometrial keratins are unknown, these proteins serve as major structural elements of epithelial cells, where they act as a protective scaffold against mechanical and chemical stressors [75]. Evidence of increased porcine endometrial *KRT23* expression on PxD 12 [21] suggested a role for this keratin

Table 4. Top 10 enriched biological processes associated with endometrial miRNA–mRNA interactions in high versus low iCrit gilts on PxD 13 identified by DAVID functional annotation analysis.

Functional terms of overrepresented biological processes[a]	Enrichment Score[b]
Developmental maturation (5)	2.36
Pathway-restricted SMAD protein phosphorylation (3)	1.89
Regulation of pathway-restricted SMAD protein phosphorylation (3)	1.89
Regulation of thyroid hormone generation (2)	1.85
Positive regulation of metabolic process (16)	1.74
Cell development (12)	1.72
Double-strand break repair (4)	1.70
Negative regulation of cell migration (4)	1.66
Metanephros development (3)	1.59
Negative regulation of cell motility (4)	1.59

[a]Values within parentheses indicate the number of annotated mRNAs targeted by miRNAs that are involved with the corresponding functional term.

[b]Enrichment scores were determined by calculating geometric means of *P*-values involved in corresponding biological processes (in $-\log_{10}$ scale).

during the periattachment period. Data indicating reduced endometrial expression of eight different keratins in lactocrine-deficient gilts on PxD 13 suggest that functional studies of these gene products during the periattachment period are warranted.

Endometrial miRNA and miRNA–mRNA interactions

MicroRNAs target mRNAs and regulate their stability [27]. A lactocrine-sensitive uterine miRNA–mRNA interactome was recently described for the neonatal pig [9]. Two of six lactocrine-sensitive endometrial miRNAs, miR-338 and miR-144, were described for human chorioamniotic tissues and implicated in regulation of prostaglandin synthesis [76, 77]. Actions of miR-338 were proposed to be mediated through phospholipase transcript *PLA2G4B* [76]. Here, phospholipase A2 family members *PLA2G2D* and *PLA2G3* were determined to be lactocrine sensitive. However, functional roles for the five annotated, lactocrine-sensitive miRNAs predicted to target 62 mRNAs in the adult porcine endometrium on PxD 13 are unknown.

Summary

Data for the uterus, generated in rodent and ungulate models, including cattle, sheep, and pigs, indicate that targeted disruption of uterine development from birth can alter the neonatal developmental program with lasting, and typically negative consequences for uterine phenotype and function in adulthood [1]. Data for the pig indicate that lactocrine effects on the neonatal porcine uterine developmental program occur rapidly, within the first 12 to 24 h of birth [9, 78]. Given that lactocrine deficiency from birth predicts permanent impairment of reproductive performance in female pigs [14], observations suggest that the first 12 to 24 h of neonatal life define a critical period for lactocrine programming of porcine uterine development and function [7, 8]. It is now important to define epigenetic lactocrine programming mechanisms regulating uterine development [8, 79].

Epigenetic mechanisms implicated in developmental programming include DNA methylation, post-translational histone modifications, and miRNA-mediated effects on transcript stability and repression of translation during critical organizational periods [80]. Data for the pig, indicating lactocrine effects on aspects of the neonatal uterine miRNA–mRNA interactome by PND 2 [9], implicated miRNAs as elements of the lactocrine programming story. Nothing is known about roles for DNA methylation or post-translational histone modifications in this regard. Interrogation of neonatal porcine transcriptomic datasets on PND 2 [9, 10] for evidence of lactocrine-sensitive uterine expression of genes that code for enzymes regulating these processes, such as DNA methyltransferases and histone-modifying enzymes, will be instructive. To the extent that the epigenome connects genotype to phenotype, definition of lactocrine mechanisms mediating development and, ultimately, tissue function will be important for understanding developmental origins of mammalian health and disease, including reproductive performance. Evidence for the pig indicates that adequate colostrum consumption within 24 hours of birth is required for establishment of a normal uterine developmental program and optimal reproductive performance in adults.

Supplementary data

Supplementary data are available at *BIOLRE* online.

Supplemental Table S1. Summary of alignment statistics for mRNAseq of endometrial samples from high and low iCrit gilts on PxD 13.
Supplemental Table S2. Primer sequences for quantitative real-time PCR validation of mRNAseq.
Supplemental Table S3. Differentially expressed endometrial mRNAs ($\geq \pm 1.5$-fold change; $P < 0.05$) between high and low iCrit gilts on PxD 13.
Supplemental Table S4. Integrated target prediction analysis for differentially expressed endometrial miRNAs and mRNA targets between high and low iCrit gilts on PxD 13 as identified by Ingenuity Pathway Analysis.

Acknowledgment

The authors thank the USDA ARS Meat Animal Research Center staff for their contributions to the animal work. Additional thanks to the HudsonAlpha Genomics Services Laboratory for their contributions to the sequencing for this study. Mention of trade name, proprietary product, or specified equipment does not constitute a guarantee or warranty by the USDA and does not imply approval to the exclusion of other products that may be suitable. The USDA is an equal opportunity provider and employer.

References

1. Cooke PS, Spencer TE, Bartol FF, Hayashi K. Uterine glands: development, function and experimental model systems. *Mol Hum Reprod* 2013; **19**(9):547–558.
2. Bartol FF, Wiley AA, Floyd JG, Ott TL, Bazer FW, Gray CA, Spencer TE. Uterine differentiation as a foundation for subsequent fertility. *J Reprod Fertil Suppl* 1999; **54**:287–302.
3. Bartol FF, Wiley AA, Coleman DA, Wolfe DF, Riddell MG. Ovine uterine morphogenesis: effects of age and progestin administration and withdrawal on neonatal endometrial development and DNA synthesis. *J Anim Sci* 1988; **66**(11):3000–3009.
4. Gray CA, Taylor KM, Ramsey WS, Hill JR, Bazer FW, Bartol FF, Spencer TE. Endometrial glands are required for preimplantation conceptus elongation and survival. *Biol Reprod* 2001; **64**(6):1608–1613.
5. Cooke PS, Ekman GC, Kaur J, Davila J, Bagchi IC, Clark SG, Dziuk PJ, Hayashi K, Bartol FF. Brief exposure to progesterone during a critical neonatal window prevents uterine gland formation in mice. *Biol Reprod* 2012; **86**(3):63.

6. Filant J, Zhou H, Spencer TE. Progesterone inhibits uterine gland development in the neonatal mouse uterus. *Biol Reprod* 2012; **86**(5):146, 141–149.
7. Bagnell CA, Ho TY, George AF, Wiley AA, Miller DJ, Bartol FF. Maternal lactocrine programming of porcine reproductive tract development. *Mol Reprod Dev* 2017; **84**(9):957–968.
8. Bartol FF, Wiley AA, George AF, Miller DJ, Bagnell CA. Physiology and endocrinology symposium: postnatal reproductive development and the lactocrine hypothesis. *J Anim Sci* 2017; **95**:2200–2210.
9. George AF, Rahman KM, Camp ME, Prasad N, Bartol FF, Bagnell CA. Defining age- and lactocrine-sensitive elements of the neonatal porcine uterine microRNA-mRNA interactome. *Biol Reprod* 2017; **96**(2):327–340.
10. Rahman KM, Camp ME, Prasad N, McNeel AK, Levy SE, Bartol FF, Bagnell CA. Age and nursing affect the neonatal porcine uterine transcriptome. *Biol Reprod* 2016; **94**(2):46.
11. Miller DJ, Wiley AA, Chen JC, Bagnell CA, Bartol FF. Nursing for 48 hours from birth supports porcine uterine gland development and endometrial cell compartment-specific gene expression. *Biol Reprod* 2013; **88**(1):4.
12. Wu WZ, Wang XQ, Wu GY, Kim SW, Chen F, Wang JJ. Differential composition of proteomes in sow colostrum and milk from anterior and posterior mammary glands1. *J Anim Sci* 2010; **88**(8):2657–2664.
13. Kraeling RR, Webel SK. Current strategies for reproductive management of gilts and sows in North America. *J Animal Sci Biotechnol* 2015; **6**(1):3.
14. Vallet JL, Miles JR, Rempel LA, Nonneman DJ, Lents CA. Relationships between day one piglet serum immunoglobulin immunocrit and subsequent growth, puberty attainment, litter size, and lactation performance. *J Anim Sci* 2015; **93**(6):2722–2729.
15. Vallet JL, Miles JR, Rempel LA. A simple novel measure of passive transfer of maternal immunoglobulin is predictive of preweaning mortality in piglets. *Vet J* 2013; **195**(1):91–97.
16. Bazer FW, Spencer TE, Johnson GA, Burghardt RC. Uterine receptivity to implantation of blastocysts in mammals. *Front Biosci* 2011; **3**(2):745–767.
17. Burghardt RC, Bowen JA, Newton GR, Bazer FW. Extracellular matrix and the implantation cascade in pigs. *J Reprod Fertil Suppl* 1997; **52**:151–164.
18. Geisert RD, Whyte JJ, Meyer AE, Mathew DJ, Juarez MR, Lucy MC, Prather RS, Spencer TE. Rapid conceptus elongation in the pig: An interleukin 1 beta 2 and estrogen-regulated phenomenon. *Mol Reprod Dev* 2017; **84**(9):760–774.
19. Waclawik A, Kaczmarek MM, Blitek A, Kaczynski P, Ziecik AJ. Embryo-maternal dialogue during pregnancy establishment and implantation in the pig. *Mol Reprod Dev* 2017; **84**(9):842–855.
20. Samborski A, Graf A, Krebs S, Kessler B, Bauersachs S. Deep sequencing of the porcine endometrial transcriptome on day 14 of pregnancy. *Biol Reprod* 2013; **88**(4):84.
21. Samborski A, Graf A, Krebs S, Kessler B, Reichenbach M, Reichenbach HD, Ulbrich SE, Bauersachs S. Transcriptome changes in the porcine endometrium during the preattachment phase. *Biol Reprod* 2013; **89**(6):134.
22. Bidarimath M, Edwards AK, Wessels JM, Khalaj K, Kridli RT, Tayade C. Distinct microRNA expression in endometrial lymphocytes, endometrium, and trophoblast during spontaneous porcine fetal loss. *J Reprod Immunol* 2015; **107**:64–79.
23. Cordoba S, Balcells I, Castello A, Ovilo C, Noguera JL, Timoneda O, Sanchez A. Endometrial gene expression profile of pregnant sows with extreme phenotypes for reproductive efficiency. *Sci Rep* 2015; **5**(1):14416.
24. Krawczynski K, Bauersachs S, Reliszko ZP, Graf A, Kaczmarek MM. Expression of microRNAs and isomiRs in the porcine endometrium: implications for gene regulation at the maternal-conceptus interface. *BMC Genomics* 2015; **16**(1):906.
25. Wang Y, Hu T, Wu L, Liu X, Xue S, Lei M. Identification of non-coding and coding RNAs in porcine endometrium. *Genomics* 2017; **109**(1):43–50.
26. Wang Y, Xue S, Liu X, Liu H, Hu T, Qiu X, Zhang J, Lei M. Analyses of long non-coding RNA and mRNA profiling using RNA sequencing during the pre-implantation phases in pig endometrium. *Sci Rep* 2016; **6**(1):20238.
27. Bartel DP. MicroRNAs: genomics, biogenesis, mechanism, and function. *Cell* 2004; **116**(2):281–297.
28. Vallet JL, Miles JR. The effect of farrowing induction on colostrum and piglet serum immunocrits is dependent on parity. *J Anim Sci* 2017; **95**:688–696.
29. Rak A, Drwal E, Karpeta A, Gregoraszczuk EL. Regulatory role of gonadotropins and local factors produced by ovarian follicles on in vitro resistin expression and action on porcine follicular steroidogenesis. *Biol Reprod* 2015; **92**(6):142.
30. Robinson MD, Oshlack A. A scaling normalization method for differential expression analysis of RNA-seq data. *Genome Biol* 2010; **11**(3):R25.
31. Tatusov RL, Koonin EV, Lipman DJ. A genomic perspective on protein families. *Science* 1997; **278**(5338):631–637.
32. Griffiths-Jones S. The microRNA registry. *Nucleic Acids Res* 2004; **32**(90001):109D–111.
33. Griffiths-Jones S, Grocock RJ, van Dongen S, Bateman A, Enright AJ. miRBase: microRNA sequences, targets and gene nomenclature. *Nucleic Acids Res* 2006; **34**(90001):D140–D144.
34. Griffiths-Jones S, Saini HK, van Dongen S, Enright AJ. miRBase: tools for microRNA genomics. *Nucleic Acids Res* 2008; **36**(Database):D154–D158.
35. Kozomara A, Griffiths-Jones S. miRBase: integrating microRNA annotation and deep-sequencing data. *Nucleic Acids Res* 2011; **39**(Database):D152–D157.
36. Kozomara A, Griffiths-Jones S. miRBase: annotating high confidence microRNAs using deep sequencing data. *Nucleic Acids Res* 2014; **42**(D1):D68–D73.
37. Huang da W, Sherman BT, Lempicki RA. Systematic and integrative analysis of large gene lists using DAVID bioinformatics resources. *Nat Protoc* 2009; **4**(1):44–57.
38. Huang da W, Sherman BT, Lempicki RA. Bioinformatics enrichment tools: paths toward the comprehensive functional analysis of large gene lists. *Nucleic Acids Res* 2009; **37**(1):1–13.
39. Mi H, Huang X, Muruganujan A, Tang H, Mills C, Kang D, Thomas PD. PANTHER version 11: expanded annotation data from Gene Ontology and Reactome pathways, and data analysis tool enhancements. *Nucleic Acids Res* 2017; **45**(D1):D183–D189.
40. Chen JC, Wiley AA, Ho TY, Frankshun AL, Hord KM, Bartol FF, Bagnell CA. Transient estrogen exposure from birth affects uterine expression of developmental markers in neonatal gilts with lasting consequences in pregnant adults. *Reproduction* 2010; **139**(3):623–630.
41. Bartol FF, Wiley AA, Bagnell CA. Epigenetic programming of porcine endometrial function and the lactocrine hypothesis. *Reprod Domest Anim* 2008; **43**(Suppl 2):273–279.
42. Gutierrez K, Dicks N, Glanzner WG, Agellon LB, Bordignon V. Efficacy of the porcine species in biomedical research. *Front Genet* 2015; **6**:293.
43. Bazer FW, Kim J, Ka H, Johnson GA, Wu G, Song G. Select nutrients in the uterine lumen of sheep and pigs affect conceptus development. *J Reprod Dev* 2012; **58**:180–188.
44. Zavy MT, Clark WR, Sharp DC, Roberts RM, Bazer FW. Comparison of glucose, fructose, ascorbic acid and glucosephosphate lsomerase enzymatic activity in uterine flushings from nonpregnant and pregnant guts and pony mares. *Biol Reprod* 1982; **27**:1147–1158.
45. Vallet JL, McNeel AK, Miles JR, Freking BA. Placental accommodations for transport and metabolism during intra-uterine crowding in pigs. *J Anim Sci Biotechnol* 2014; **5**:55.
46. Steinhauser CB, Landers M, Myatt L, Burghardt RC, Vallet JL, Bazer FW, Johnson GA. Fructose synthesis and transport at the uterine-placental interface of pigs: cell-specific localization of SLC2A5, SLC2A8, and components of the polyol pathway. *Biol Reprod* 2016; **95**:108–108.
47. Steinhauser CB, Wing TT, Gao H, Li X, Burghardt RC, Wu G, Bazer FW, Johnson GA. Identification of appropriate reference genes for qPCR analyses of placental expression of SLC7A3 and induction of SLC5A1 in porcine endometrium. *Placenta* 2017; **52**:1–9.

48. Wright EM. Glucose transport families SLC5 and SLC50. *Mol Aspects Med* 2013; **34**:183–196.
49. Goldstein MH, Bazer FW, Barron DH. Characterization of changes in volume, osmolarity and electrolyte composition of porcine fetal fluids during gestation. *Biol Reprod* 1980; **22**:1168–1180.
50. Seo H, Choi Y, Shim J, Yoo I, Ka H. Comprehensive analysis of prostaglandin metabolic enzyme expression during pregnancy and the characterization of AKR1B1 as a prostaglandin f synthase at the maternal-conceptus interface in pigs. *Biol Reprod* 2014; **90**:99.
51. Bazer FW, Johnson GA. Pig blastocyst-uterine interactions. *Differentiation* 2014; **87**:52–65.
52. Seo H, Choi Y, Shim J, Yoo I, Ka H. Prostaglandin transporters ABCC4 and SLCO2A1 in the uterine endometrium and conceptus during pregnancy in pigs. *Biol Reprod* 2014; **90**:100–100.
53. Griffith OW, Chavan AR, Protopapas S, Maziarz J, Romero R, Wagner GP. Embryo implantation evolved from an ancestral inflammatory attachment reaction. *Proc Natl Acad Sci USA* 2017; **114**:E6566–E6575.
54. Swangchan-Uthai T, Chen Q, Kirton SE, Fenwick MA, Cheng Z, Patton J, Fouladi-Nashta AA, Wathes DC. Influence of energy balance on the antimicrobial peptides S100A8 and S100A9 in the endometrium of the post-partum dairy cow. *Reproduction* 2013; **145**:527–539.
55. Han J, Gu MJ, Yoo I, Choi Y, Jang H, Kim M, Yun CH, Ka H. Analysis of cysteine-X-cysteine motif chemokine ligands 9, 10, and 11, their receptor CXCR3, and their possible role on the recruitment of immune cells at the maternal-conceptus interface in pigs. *Biol Reprod* 2017; **97**:69–80.
56. Fouladi-Nashta AA, Mohamet L, Heath JK, Kimber SJ. Interleukin 1 signaling is regulated by leukemia inhibitory factor (LIF) and is aberrant in Lif-/- mouse uterus. *Biol Reprod* 2008; **79**:142–153.
57. Blitek A, Morawska E, Ziecik AJ. Regulation of expression and role of leukemia inhibitory factor and interleukin-6 in the uterus of early pregnant pigs. *Theriogenology* 2012; **78**:951–964.
58. Stewart CL, Kaspar P, Brunet LJ, Bhatt H, Gadi I, Kontgen F, Abbondanzo SJ. Blastocyst implantation depends on maternal expression of leukaemia inhibitory factor. *Nature* 1992; **359**:76–79.
59. Geisert RD, Pratt TN, Bazer FW, Mayes JS, Watson GH. Immunocytochemical localization and changes in endometrial progestin receptor protein during the porcine oestrous cycle and early pregnancy. *Reprod Fertil Dev* 1994; **6**:749–760.
60. Geisert RD, Brenner RM, Moffatt RJ, Harney JP, Yellin T, Bazer FW. Changes in oestrogen receptor protein, mRNA expression and localization in the endometrium of cyclic and pregnant gilts. *Reprod Fertil Dev* 1993; **5**:247–260.
61. Seo H, Kim M, Choi Y, Lee CK, Ka H. Analysis of lysophosphatidic acid (LPA) receptor and LPA-induced endometrial prostaglandin-endoperoxide synthase 2 expression in the porcine uterus. *Endocrinology* 2008; **149**:6166–6175.
62. Song G, Dunlap KA, Kim J, Bailey DW, Spencer TE, Burghardt RC, Wagner GF, Johnson GA, Bazer FW. Stanniocalcin 1 is a luminal epithelial marker for implantation in pigs regulated by progesterone and estradiol. *Endocrinology* 2009; **150**:936–945.
63. Cheon YP, Xu X, Bagchi MK, Bagchi IC. Immune-responsive gene 1 is a novel target of progesterone receptor and plays a critical role during implantation in the mouse. *Endocrinology* 2003; **144**:5623–5630.
64. Li J, Liu WM, Cao YJ, Peng S, Zhang Y, Duan EK. Roles of Dickkopf-1 and its receptor Kremen1 during embryonic implantation in mice. *Fertil Steril* 2008; **90**:1470–1479.
65. Lee KY, Jeong JW, Wang J, Ma L, Martin JF, Tsai SY, Lydon JP, DeMayo FJ. Bmp2 is critical for the murine uterine decidual response. *Mol Cell Biol* 2007; **27**:5468–5478.
66. Geisert RD, Johnson GA, Burghardt RC. Implantation and establishment of pregnancy in the pig. *Adv Anat Embryol Cell Biol* 2015; **216**:137–163.
67. Kufe DW. Mucins in cancer: function, prognosis and therapy. *Nat Rev Cancer* 2009; **9**:874–885.
68. Linden SK, Sutton P, Karlsson NG, Korolik V, McGuckin MA. Mucins in the mucosal barrier to infection. *Mucosal Immunol* 2008; **1**:183–197.
69. Poon CE, Lecce L, Day ML, Murphy CR. Mucin 15 is lost but mucin 13 remains in uterine luminal epithelial cells and the blastocyst at the time of implantation in the rat. *Reprod Fertil Dev* 2014; **26**:421–431.
70. Forde N, Mehta JP, McGettigan PA, Mamo S, Bazer FW, Spencer TE, Lonergan P. Alterations in expression of endometrial genes coding for proteins secreted into the uterine lumen during conceptus elongation in cattle. *BMC Genomics* 2013; **14**:321.
71. Bowen JA, Bazer FW, Burghardt RC. Spatial and temporal analyses of integrin and muc-1 expression in porcine uterine epithelium and trophectoderm in vivo. *Biol Reprod* 1996; **55**:1098–1106.
72. Ferrell AD, Malayer JR, Carraway KL, Geisert RD. Sialomucin complex (Muc4) expression in porcine endometrium during the oestrous cycle and early pregnancy. *Reprod Domest Anim* 2003; **38**:63–65.
73. Curry TE, Jr, Osteen KG. The matrix metalloproteinase system: changes, regulation, and impact throughout the ovarian and uterine reproductive cycle. *Endocr Rev* 2003; **24**:428–465.
74. Weber S, Saftig P. Ectodomain shedding and ADAMs in development. *Development* 2012; **139**:3693–3709.
75. Coulombe PA, Omary MB. 'Hard' and 'soft' principles defining the structure, function and regulation of keratin intermediate filaments. *Curr Opin Cell Biol* 2002; **14**:110–122.
76. Montenegro D, Romero R, Kim SS, Tarca AL, Draghici S, Kusanovic JP, Kim JS, Lee DC, Erez O, Gotsch F, Hassan SS, Kim CJ. Expression patterns of microRNAs in the chorioamniotic membranes: a role for microRNAs in human pregnancy and parturition. *J Pathol* 2009; **217**:113–121.
77. Li H, Zhou J, Wei X, Chen R, Geng J, Zheng R, Chai J, Li F, Jiang S. miR-144 and targets, c-fos and cyclooxygenase-2 (COX2), modulate synthesis of PGE2 in the amnion during pregnancy and labor. *Sci Rep* 2016; **6**:27914.
78. Ho TY, Rahman KM, Camp ME, Wiley AA, Bartol FF, Bagnell CA. Timing and duration of nursing from birth affect neonatal porcine uterine matrix metalloproteinase 9 and tissue inhibitor of metalloproteinase 1. *Domest Anim Endocrinol* 2017; **59**:1–10.
79. Bartol FF, Wiley AA, Miller DJ, Silva AJ, Roberts KE, Davolt ML, Chen JC, Frankshun AL, Camp ME, Rahman KM, Vallet JL, Bagnell CA. Lactation biology symposium: Lactocrine signaling and developmental programming. *J Anim Sci* 2013; **91**:696–705.
80. Hoffman DJ, Reynolds RM, Hardy DB. Developmental origins of health and disease: current knowledge and potential mechanisms. *Nutr Rev* 2017; **75**:951–970.